Model for the Architecture of Claudin-Based Paracellular Ion Channels through Tight Junctions

Hiroshi Suzuki[1,†], Kazutoshi Tani[1,†], Atsushi Tamura[2], Sachiko Tsukita[2] and Yoshinori Fujiyoshi[1,3]

1 - Cellular and Structural Physiology Institute, *Nagoya University, Chikusa, Nagoya 464-8601, Japan*
2 - Laboratory of Biological Science, *Graduate School of Frontier Biosciences and Graduate School of Medicine, Osaka University, Suita, Osaka 565-0871, Japan*
3 - Department of Basic Medical Science, *Graduate School of Pharmaceutical Science, Nagoya University, Chikusa, Nagoya 464-8601, Japan*

Correspondence to Sachiko Tsukita and Yoshinori Fujiyoshi: *Sachiko Tsukita is to be contacted at : Laboratory of Biological Science, Graduate School of Frontier Biosciences and Graduate School of Medicine, Osaka University, Suita, Osaka 565-0871, Japan; Y. Fujiyoshi is to be contacted at: Cellular and Structural Physiology Institute, Nagoya University, Chikusa, Nagoya 464-8601, Japan. atsukia@biosci.med.osaka-u.ac.jp; yoshi@cespi.nagoya-u.ac.jp.*
http://dx.doi.org/10.1016/j.jmb.2014.10.020
Edited by J. Bowie

Abstract

Claudins are main cell–cell adhesion molecules of tight junctions (TJs) between cells in epithelial sheets that form tight barriers that separate the apical from the basolateral space but also contain paracellular channels that regulate the flow of ions and solutes in between these intercellular spaces. Recently, the first crystal structure of a claudin was determined, that of claudin-15, which indicated the parts of the large extracellular domains that likely form the pore-lining surfaces of the paracellular channels. However, the crystal structure did not show how claudin molecules are arranged in the cell membrane to form the backbone of TJ strands and to mediate interactions between adjacent cells, information that is essential to understand how the paracellular channels in TJs function. Here, we propose that TJ strands consist of claudin protomers that assemble into antiparallel double rows. This model is based on cysteine crosslinking experiments that show claudin-15 to dimerize face to face through interactions between the edges of the extracellular β-sheets. Strands observed by freeze-fracture electron microscopy of TJs also show that their width is consistent with the dimensions of a claudin dimer. Furthermore, we propose that extracellular variable regions are responsible for head-to-head interactions of TJ strands in adjoining cells, thus resulting in the formation of paracellular channels. Our model of the TJ architecture provides a basis to discuss structural mechanisms underlying the selective ion permeability and barrier properties of TJs.

Introduction

The apical-most region of lateral cell membranes in epithelial cell sheets is circumscribed by a belt-like meshwork structure, known as tight junctions (TJs) [1–3]. TJs completely occlude spaces between adjoining epithelial cells but they also contain paracellular channels that tightly regulate the solute flow through intercellular spaces of epithelial cell sheets, thus maintaining various internal compartments of our bodies and separating them from the external environment [4,5]. The barrier function and the permeability characteristics of epithelial cell sheets covering different organs are particularly defined by the properties of the TJs and their paracellular channels, creating the organ-specific microenvironments [6,7]. In contrast to canonical channels that form narrow, membrane-embedded pores for the transport of substances across lipid bilayers, paracellular pathways are oriented parallel with the plane of the plasma membranes, but they also possess electrophysiological properties of size-

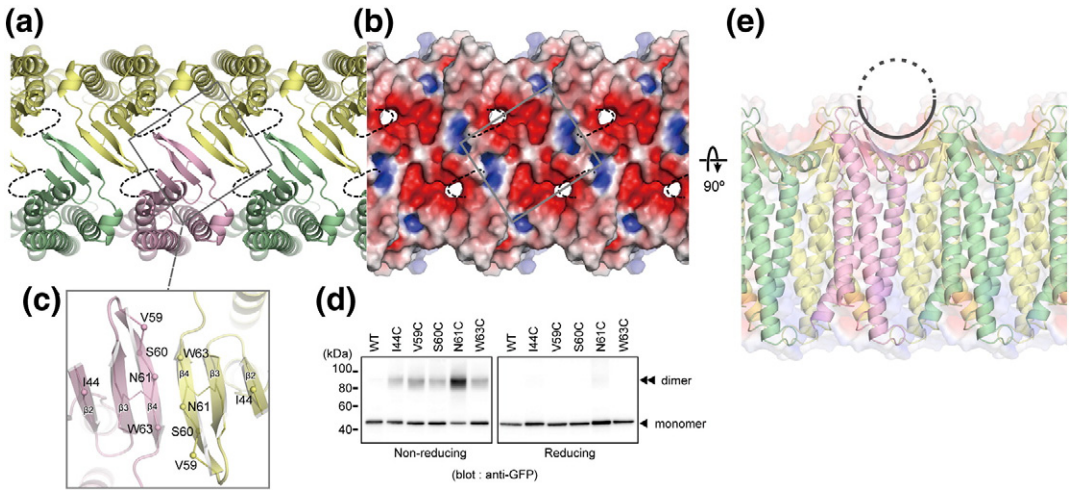

Fig. 1. Proposed arrangement of claudin protomers in TJ strands. (a and b) Model of an antiparallel double row of claudin molecules viewed from the extracellular side. The mCldn15 protomers (PDB entry: 4P79) are shown in ribbon representation (a) and as electrostatic potential surface contoured from −4 *kT*/*e* (red) to +4 *kT*/*e* (blue), calculated with the Adaptive Poisson–Boltzmann Solver [32] (b) Broken lines indicate the disordered loop in ECS1. (c) Close-up view of the interface between the modeled mCldn15 dimer. Spheres indicate the C^{α} positions of the labeled residues. (d) Western blot analysis of spontaneous crosslinking of ECFP-claudin-15 constructs containing cysteine substitutions in the β-sheet domain. (e) Side view of the double-row claudin arrangement shown in (a) and (b). The continuous line indicates the extracellular "half pipe" structure formed by the shown claudin dimer, and the broken line indicates the putative another "half pipe" in an adjacent cell to complete the channel. Transmembrane contacts can be seen on the surface of the side view of the TJ model.

limiting pores with charge and relative ion selectivity [7].

TJs consist of a meshwork of linear strands, which are predominantly formed by claudins, a family of four-transmembrane proteins with 27 members in human and mouse. The physiological properties of TJs mainly depend on the specific subtypes of claudins they contain [8–11]. While TJs also contain other membrane and scaffold proteins, claudin alone can reconstitute TJ-like meshwork strands in plasma membranes at cell–cell contact planes, suggesting that claudins form the backbone of TJ strands [12]. Although previous reports have unambiguously shown that residues in the extracellular domains of claudins are involved in cell adhesion and affect the permeability and charge selectivity of the paracellular pathways [13–17], the molecular arrangement of claudins in TJ strands and the structural basis for the physiological properties of paracellular channels in TJs remain unclear.

Recently, we solved the crystal structure of mouse claudin-15 (mCldn15), which formed linear, single rows in the crystal [18]. The structure revealed that the transmembrane segments (TM1–TM4) form a tight four-helix bundle and that parts of the first and second extracellular segments (ECS1 and ECS2) form a domain with a unique β-sheet fold. Five extracellular β-strands (β1–β5) form a "palm"-shaped structure that is likely to form the pore-lining surfaces of the paracellular ion pathways. Although the linear alignment of the protomers in the crystal likely reflects the way claudins polymerize to form TJ strands (see details in Ref. [18]), the crystals did not show higher-order assemblies that would explain the architecture of paracellular pathways across TJ strands.

Here, we present a model for the architecture of TJ strands, which is based on linear claudin polymers assembling within the membrane into antiparallel double rows. This model is supported by results of crosslinking experiments and by electron microscopic images showing that a double-row arrangement of claudin molecules is consistent with the width of TJ strands. Furthermore, association of antiparallel claudin double rows in adjacent membranes would result in extracellular β-barrel-like pores that could be the paracellular pathways parallel with the membrane plane.

Results and discussion

Side-by-side interaction of claudins in a TJ strand

The recently solved crystal structure of mCldn15 showed that negatively charged residues responsible for the cation selectivity are part of the extracellular β-sheet domain and locate to one side of the linear polymer that resembles the teeth of a saw blade [18]. We speculated that a second linear polymer could associate in an antiparallel fashion, leading to a model in which TJ strands are formed by mCldn15 molecules arranged in an antiparallel

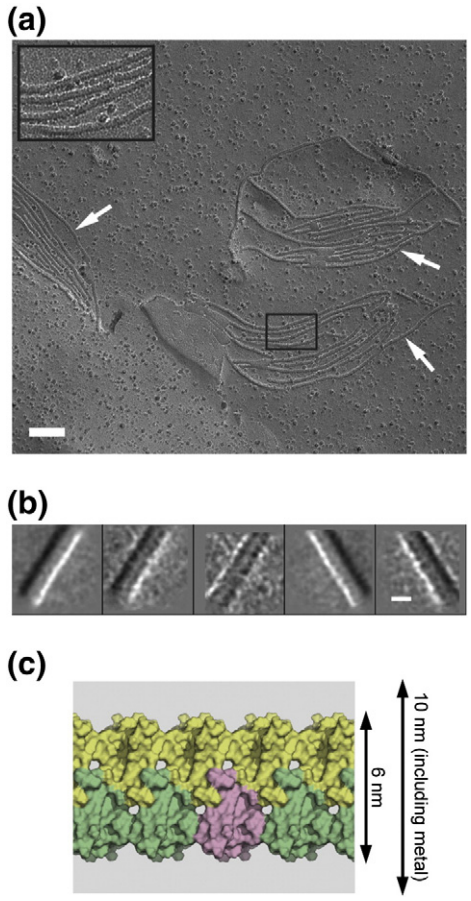

Fig. 2. Electron microscopy of freeze-fracture replicas and single-particle analysis of TJ-like strands. (a) A representative electron micrograph of a freeze-fracture replica showing the P-face of the plasma membrane of fixed Sf9 insect cells expressing a mouse claudin-15 construct with an N-terminal EGFP fusion. The arrows point to TJ-like strands. The inset shows a magnified view of the boxed area. The scale bar represents 100 nm. (b) Two-dimensional class averages calculated with segments windowed from straight regions of TJ-like strands. The scale bar represents 10 nm. (c) Space-filling model of the antiparallel double-row arrangement of claudin protomers. The height of the gray panel indicates the width of the strand including the metal layer deposited by rotary platinum shadowing.

double row (Fig. 1a and b). In this model, mCldn15 molecules in the two strands interact with each other through their β-sheet domains, allowing the formation of hydrogen bonds and resulting in a continuous antiparallel β-sheet structure, which would be energetically favorable and stable.

To test this model, we introduced cysteine residues at the putative interface between claudins in the two rows (Fig. 1c) and analyzed the expressed protein by gel electrophoresis under non-reducing conditions. A single cysteine substitution at Asn61 resulted in a major shift of the expressed protein to a position consistent with a dimer (Fig. 1d). Other cysteine substitutions also resulted in weak dimer bands. However, since even Ile44 shows a slight tendency to dimerize despite its side chain being occluded in the core of the extracellular domain, we assign these weaker dimer signals to be due to background crosslinking resulting from the transient expression of the mutants. In the presence of a reducing agent, all mutants migrated at the position of monomeric wild-type protein (Fig. 1d). The observation that the N61C mutant forms dimers supports the notion that mCldn15 molecules form face-to-face homodimers, in which the Asn61 residues of two protomers are in close proximity, consistent with the antiparallel double-row model that is stabilized by interactions through the β-sheet domains as shown in Fig. 1c. The dimeric interactions should occur between protomers in the same membrane because the disulfide crosslinking occurred by transient expression in HEK293 cells and did not depend on the assembly of mCldn15 into TJs in cell–cell contact regions. In the proposed antiparallel double-row arrangement of claudin protomers, the interaction of the extracellular "palms" of mCldn15 protomers in the two rows results in the formation of a "half pipe"-shaped structure across the antiparallel double row (Fig. 1e), which has a negatively charged surface (Fig. 1b). This "half pipe" would likely provide a route for the paracellular pathway.

Freeze-fracture electron microscopy of TJ strands

Early freeze-fracture electron microscopy studies of *in vivo* TJs revealed continuous TJ strands that have a diameter similar to the width of our model of claudin protomers arranged in an antiparallel double row [2]. To estimate the precise width of TJ-like strands in cell membranes, we expressed claudin-15 fused to enhanced green fluorescent protein (EGFP) in Sf9 insect cells and analyzed the plasma membranes by freeze-fracture electron microscopy and rotary shadowing with platinum (Fig. 2a). The cell membranes showed prominent TJ-like strands, and because the fractured membranes were prepared by rotary shadowing, platinum was deposited almost equally around the strands irrespective of their direction. Straight regions of the strands were then selected to extract small segments that were aligned to each other and classified into five groups to calculate projection averages (Fig. 2b). The width of the averaged strands was 9.7 ± 4.1 nm, which is consistent with that of the modeled claudin double row (approximately 6.0 nm), taking into account the artificial thickening of the strand resulting from the deposition of approximately 2 nm of metal on both sides of the strand (Figs. 1a,b and 2c). Therefore, the averages support our model that TJ strands in adjoining membranes are formed by antiparallel double rows of claudin protomers.

Model for the paracellular pores in TJ strands

TJs assemble through homotypic and heterotypic *cis*- and *trans*-interactions between claudins, in

which the two extracellular segments serve distinct but cooperative functions [16]. Residues in ECS1 were proposed to participate in the formation of the paracellular pathway and to determine its charge selectivity [16,17,19], while residues in ECS2 were reported to contribute to *trans*-interactions between claudin molecules of adjacent cells [20,21]. We previously defined poorly conserved loop regions in ECS1 and ECS2 as variable regions V1 and V2, respectively, and homology models of claudins indicated that these regions are part of flexible loops (Fig. S1a) [18]. It is conceivable that the diversity of the flexible regions is responsible for making sure that only subtypes in the claudin family that are compatible with each other can interact with each other to form junctions [13,16], thus playing a critical role in TJ function.

Considering that the V1 and V2 regions are located at the two sides of the “half pipe” formed by the β-sheet domains in the modeled TJ strand (Fig. S1b and c), these regions of claudin molecules in adjacent cells may change their conformation to engage in *trans*-interactions with each other through an induced fit, thus functioning as "pillars" that support the space needed for the formation of paracellular pathways. The “half pipe” architecture depicted in Fig. 1e suggests that the joining of two claudin double rows in adjoining cells would result in the formation of a complete “β-sheet channel” across the TJ (Fig. 3a and b). The distance between the two adjacent cell membranes deduced from the model is in good agreement with the distance between membranes in TJs observed by thin-section electron microscopy [1]. In addition, between the two “half pipe” structures, there is enough space to accommodate the disordered V1 region, Val34-Thr41, in the crystal structure (Fig. 3b and S1b), and thus, the V1 region will not likely prevent these two structures from docking to form the TJ architecture. The resulting pore of the “β-sheet channel” would have a diameter of less than 10 Å, consistent with previous observations [9], and thus, it would not only permeate hydrated ions but also restrict their diffusion depending on the configuration of pore-lining residues [22,23]. Continuous adhesion along the TJ strand would result in the formation of a row of channels in the space between interacting cells (Fig. 4a). The β-barrel-like structure of the pore would be an effective scaffold to line the pathway with desired residues because the geometric restrictions of the β-sheet structure will result in the side chains pointing into the interior of the pore. The proposed paracellular pathway in TJs is clearly distinct from the conventional transcellular pathway in gap junctions, as solutes in the former flow parallel and in between two adjacent membranes (Fig. 4a), whereas in the latter, they flow perpendicular and across two adjacent membranes (Fig. 4b) [24]. Both types of junctions have long pathways and narrow constriction sites in the channels so that they could function as ion permeation channels and high-resistance barriers to any solutes by changing even one narrow constriction site.

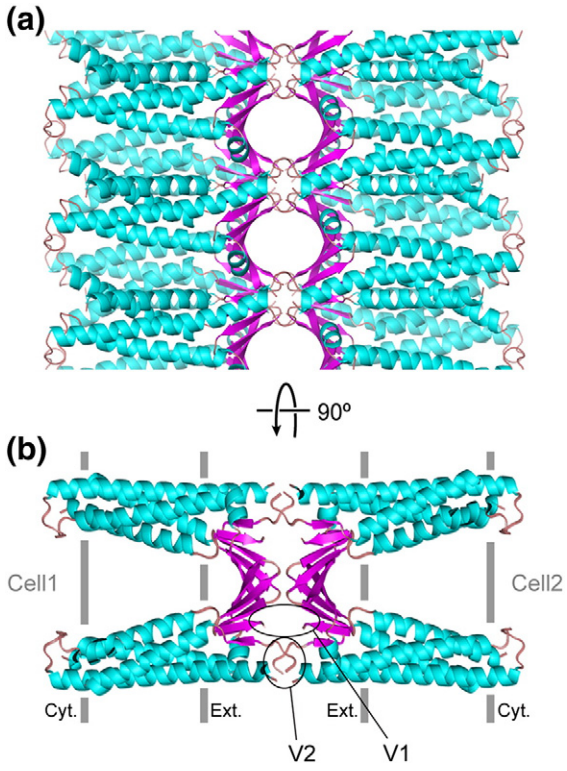

Fig. 3. Proposed model of paracellular TJ channels shown in ribbon representation. The “β-sheet channels” resulting from the proposed arrangement of claudin protomers, viewed perpendicular to (a) and parallel with (b) the elongation direction of the TJ strand. The V1 and V2 regions are circled in (b). Disordered loops and regions that caused steric clashes in the model are not shown. The proposed structural model and the movie can be downloaded as supplementary data.

Claudin-15 is a predominantly channel-forming claudin subtype, and when exogenously expressed in epithelial cell lines, it can form cation-selective TJs [19,25,26]. Charge-reversing mutations of acidic residues in the extracellular domain of claudin-15 (red letters in Fig. S1a) resulted in paracellular channels with the opposite ion selectivity, that is, selectivity for anions [19]. As the same effect was observed in transcellular pentameric cation and anion channels [27,28], we suggest, by analogy, that the paracellular pathway comprising claudin-15 may contain rings of negative charges that interact with permeating cations. In the modeled β-sheet channel, the four claudin protomers forming the paracellular pathway could each contribute the acidic residues responsible for cation selectivity and create the negative electrostatic potential in the inside of the pore (Figs. 1b and 4a). Intensive electrophysiological studies of claudin-2 suggested that the paracellular pores formed by this claudin are narrow (~6.5 Å in

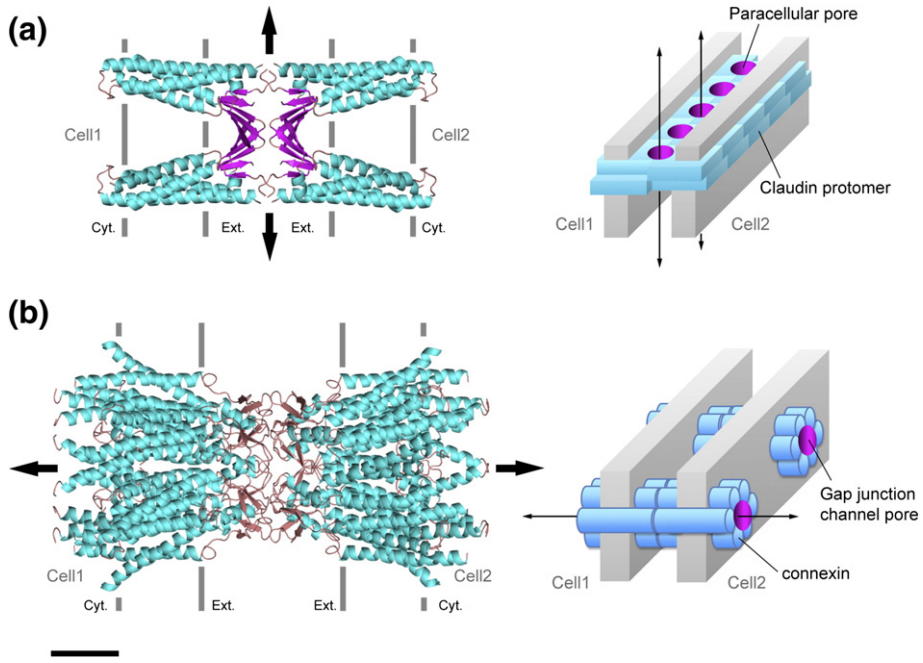

Fig. 4. Comparison of two junction-forming channels. (a) Model of the proposed paracellular ion pathways across TJs shown in ribbon representation (left) and as a schematic drawing (right), in which the putative β-sheet pores are colored magenta and the remaining claudin protomers are represented by cyan blocks. (b) Crystal structure of a gap junction channel formed by connexin 26 (PDB entry: 2ZW3) [24] shown in ribbon representation (left) and as a schematic drawing (right), in which the transcellular pores are colored magenta and the connexin protomers are represented by cyan cylinders. Gray lines and plates indicate cell membrane surfaces, and up-down or left-right double arrows indicate the pathways and directions of permeating ions. The scale bar represents 30 Å.

diameter) and possess highly negatively charged binding sites that can coordinate permeating cations in a partially dehydrated form [16,17]. Ionotropic glutamate receptor channels, which are conventional ion channels, have a similar pore diameter of 5.5–7.0 Å and permeate different hydrated or partially hydrated cations across the membrane, depending on which subunit isoforms form the tetrameric channel [29,30]. Therefore, the mechanism underlying the conduction of hydrated or partially hydrated ions through paracellular channel pores should be similar to that used by conventional ion channels, and the ion selectivity of the paracellular channels would depend on the claudin subtypes that make up the TJs. Our structural model will provide novel insights on how TJs can function both as paracellular barriers and as channels, although additional structure–function studies will be required to verify and further refine the model for the TJ architecture.

Materials and methods

Cysteine crosslinking and Western blotting

The QuikChange (Agilent Technologies) method was used to introduce cysteine substitutions into a palmitoylation-deficient mouse claudin-15 construct (C102A/C183,184,185A) in a pECFP-C1 mammalian expression vector (Clontech). Effectene Reagent (QIAGEN) was used to transiently transfect HEK293 cells, which were sparsely cultured in Dulbecco's modified Eagle's medium supplemented with 10% fetal bovine serum. Cells were harvested 48 h after transfection and solubilized with 2% *n*-dodecyl-β-D-maltopyranoside in 50 mM Tris–HCl (pH 7.5), 150 mM NaCl, and 1 mM ethylenediaminetetraacetic acid, containing protease inhibitor cocktail (Nacalai, Kyoto, Japan). After ultracentrifugation at 66,000*g* for 30 min at 4 °C, the supernatant was separated by SDS-PAGE in the absence ("Non-reducing") or presence ("Reducing") of 5% (v/v) 2-mercaptoethanol. The proteins were transferred to polyvinylidene difluoride membranes, probed with anti-GFP monoclonal antibodies (Nacalai), and detected with the ECL Prime detection kit (GE Healthcare).

Freeze-fracture electron microscopy

Claudin-15 with N-terminal EGFP was expressed in Sf9 insect cells by baculovirus infection as previously described [18]. The infected cells were fixed with 2.5% glutaraldehyde in phosphate buffer (100 mM sodium phosphate, pH 7.2) for 30 min at 27 °C and were cryo-protected with 30% glycerol in phosphate buffer. Cells were frozen by immersion into liquid nitrogen, fractured in a JFD-V freeze-etching system (JEOL) at

– 120 °C, and shadowed first by rotary evaporation of platinum carbon at an angle of 60° and then by rotary evaporation of carbon from the top. Replica specimens were imaged in a JEM-1010 electron microscope (JEOL) equipped with a 4k × 4k CMOS camera (TVIPS) at a magnification of 20,000 ×.

Analysis of freeze-fracture replica images

Using EMAN Boxer [32], we selected a total of 363 non-overlapping segments of 64 × 64 pixels (6.4 Å/pixel) from approximately straight regions of TJ-like strands in electron microscopic images of freeze-fracture replicas. For the calculation of class averages, the segment images were aligned and classified into five classes using multivariate statistical analysis. All image processing was performed in EMAN.

Acknowledgements

We thank M. Uji and H. Tanaka for technical support and T. Walz for critical reading of the manuscript. This research was supported by Grants-in-Aid for Scientific Research (S) (to Y.F.) and (A) (to S.T.), Grants-in-Aid for Scientific Research on Innovative Areas (to S.T.), Grants-in-Aid for Scientific Research (C) (to K.T.), and Platform for Drug Discovery, Information, and Structural Life Science from the Ministry of Education, Culture, Sports, Science and Technology of Japan. This research was also supported by Japan Science and Technology Agency CREST (to S.T.), the Japan New Energy and Industrial Technology Development Organization, and the National Institute of Biomedical Innovation (to Y.F.).

Appendix A. Supplementary data

Supplementary data to this article can be found online at http://dx.doi.org/10.1016/j.jmb.2014.10.020.

Received 12 September 2014;
Received in revised form 24 October 2014;
Accepted 29 October 2014
Available online 4 November 2014

Keywords:
claudin;
cell adhesion;
tight junctions;
paracellular transport;
ion channels

Present address: H. Suzuki, Department of Cell Biology, Harvard Medical School, Boston, MA 02115, USA.

† H.S. and K.T. contributed equally to this work.

Abbreviations used:
TJ, tight junction; EGFP, enhanced green fluorescent protein; ECFP, enhanced cyan fluorescent protein.

References

[1] Farquhar MG, Palade GE. Junctional complexes in various epithelia. J Cell Biol 1963;17:375–412.
[2] Staehelin LA. Further observations on the fine structure of freeze-cleaved tight junctions. J Cell Sci 1973;13:763–86.
[3] Gumbiner B. Structure, biochemistry, and assembly of epithelial tight junctions. Am J Physiol 1987;253:C749–58.
[4] Frömter E, Diamond J. Route of passive ion permeation in epithelia. Nat New Biol 1972;235:9–13.
[5] Schneeberger EE, Lynch RD. Structure, function, and regulation of cellular tight junctions. Am J Physiol 1992;262:L647–61.
[6] Powell DW. Barrier function of epithelia. Am J Physiol 1981;241:G275–88.
[7] Tang VW, Goodenough DA. Paracellular ion channel at the tight junction. Biophys J 2003;84:1660–73.
[8] Tsukita S, Furuse M, Itoh M. Multifunctional strands in tight junctions. Nat Rev Mol Cell Biol 2001;2:285–93.
[9] Van Itallie CM, Anderson JM. Claudins and epithelial paracellular transport. Annu Rev Physiol 2006;68:403–29.
[10] Mineta K, Yamamoto Y, Yamazaki Y, Tanaka H, Tada Y, Saito K, et al. Predicted expansion of the claudin multigene family. FEBS Lett 2011;585:606–12.
[11] Günzel D, Yu ASL. Claudins and the modulation of tight junction permeability. Physiol Rev 2013;93:525–69.
[12] Furuse M, Sasaki H, Fujimoto K, Tsukita S. A single gene product, claudin-1 or -2, reconstitutes tight junction strands and recruits occludin in fibroblasts. J Cell Biol 1998;143:391–401.
[13] Furuse M, Sasaki H, Tsukita S. Manner of interaction of heterogeneous claudin species within and between tight junction strands. J Cell Biol 1999;147:891–903.
[14] Colegio OR, Van Itallie C, Rahner C, Anderson JM. Claudin extracellular domains determine paracellular charge selectivity and resistance but not tight junction fibril architecture. Am J Physiol Cell Physiol 2003;284:C1346–54.
[15] Van Itallie CM, Fanning AS, Anderson JM. Reversal of charge selectivity in cation or anion-selective epithelial lines by expression of different claudins. Am J Physiol Renal Physiol 2003;285:F1078–84.
[16] Angelow S, Ahlstrom R, Yu ASL. Biology of claudins. Am J Physiol Renal Physiol 2008;295:F867–76.
[17] Yu ASL, Cheng MH, Angelow S, Günzel D, Kanzawa SA, Schneeberger EE, et al. Molecular basis for cation selectivity in claudin-2-based paracellular pores: identification of an electrostatic interaction site. J Gen Physiol 2009;133:111–27.
[18] Suzuki H, Nishizawa T, Tani K, Yamazaki Y, Tamura A, Ishitani R, et al. Crystal structure of a claudin provides insight into the architecture of tight junctions. Science 2014;344:304–7.
[19] Colegio OR, Van Itallie CM, McCrea HJ, Rahner C, Anderson JM. Claudins create charge-selective channels in the paracellular pathway between epithelial cells. Am J Physiol Cell Physiol 2002;283:C142–7.
[20] Piontek J, Winkler L, Wolburg H, Müller SL, Zuleger N, Piehl C, et al. Formation of tight junction: determinants of homophilic

interaction between classic claudins. FASEB J 2008;22: 146–58.
[21] Krause G, Winkler L, Mueller SL, Haseloff RF, Piontek J, Blasig IE. Structure and function of claudins. Biochim Biophys Acta 2008;1778:631–45.
[22] Dwyer TM, Adams DJ, Hille B. The permeability of the endplate channel to organic cations in frog muscle. J Gen Physiol 1980;75:469–92.
[23] Unwin N, Fujiyoshi Y. Gating movement of acetylcholine receptor caught by plunge-freezing. J Mol Biol 2012;422: 617–34.
[24] Maeda S, Nakagawa S, Suga M, Yamashita E, Oshima A, Fujiyoshi Y, et al. Structure of the connexin 26 gap junction channel at 3.5 Å resolution. Nature 2009;458: 597–602.
[25] Inai T, Kamimura T, Hirose E, Iida H, Shibata Y. The protoplasmic or exoplasmic face association of tight junction particles cannot predict paracellular permeability or heterotypic claudin compatibility. Eur J Cell Biol 2010;89:547–56.
[26] Tamura A, Hayashi H, Imasato M, Yamazaki Y, Hagiwara A, Wada M, et al. Loss of claudin-15, but not claudin-2, causes Na^+ deficiency and glucose malabsorption in mouse small intestine. Gastroenterology 2011;140:913–23.
[27] Galzi JL, Devillers-Thiéry A, Hussy N, Bertrand S, Changeux JP, Bertrand D. Mutations in the channel domain of a neuronal nicotinic receptor convert ion selectivity from cationic to anionic. Nature 1992;359:500–5.
[28] Keramidas A, Moorhouse AJ, French CR, Schofield PR, Barry PH. M2 pore mutations convert the glycine receptor channel from being anion- to cation-selective. Biophys J 2000;79:247–59.
[29] Villarroel A, Burnashev N, Sakmann B. Dimensions of the narrow portion of a recombinant NMDA receptor channel. Biophys J 1995;68:866–75.
[30] Burnashev N, Villarroel A, Sakmann B. Dimensions and ion selectivity of recombinant AMPA and kainate receptor channels and their dependence on Q/R site residues. J Physiol 1996;496:165–73.
[31] Ludtke SJ, Baldwin PR, Chiu W. EMAN: semiautomated software for high-resolution single-particle reconstructions. J Struct Biol 1999;128:82–97.
[32] Baker NA, Sept D, Joseph S, Holst MJ, McCammon JA. Electrostatics of nanosystems: application to microtubules and the ribosome. Proc Natl Acad Sci USA 2001;98: 10037–41.